Supplementary Information:

An intelligent electrochromic film with passive radiation cooling and synergistic solar light control capabilities for display and smart windows

Zuowei Zhang [a], Xian He [a], Meina Yu [a]*, Luoning Zhang [a], Xiao Xiao[d], Cheng Zou [a, b], Yanzi Gao [a], Qian Wang [a]*, Huai Yang [a, b, c]*

[a] Institute for Advanced Materials and Technology, University of Science and Technology Beijing, Beijing, China; [b] Beijing Advanced Innovation Center for Materials Genome Engineering, University of Science and Technology Beijing, Beijing, China; [c] School of Materials Science and Engineering, Peking University, Beijing, China; [d] School of Economics and Management, University of Chinese Academy of Sciences, Beijing, 100190, China

*Corresponding author: Meina Yu, yumeina@ustb.edu.cn; Huai Yang, yanghuai@pku.edu.cn.

1. Experimental

1.1 Materials

The polyethylene glycol 200 diacrylate (PEGDA200), the lauryl methacrylate (LMA) and 2-Hydroxyethyl methacrylate (HPMA) were purchased from shanghai Aladdin Biochemical Technology Co., Ltd. The 1H,1H-pentafluoropropyl methacrylate (PFPMA) was supplied by shanghai Meryer chemical Technology Co., Ltd. The liquid crystal monomers: 4-fluoro-4'- (4-propylcyclohexyl)-1-1'-biphenyl (1F1) (T_{Cr-N} = 23.6 °C, T_{N-I} = 67.8 °C), 4-fluoro-4'- (4-propyl- [1,1'-bi (cyclohexan)]-4-yl)-1,1'-biphenyl (2F1) (T_{Cr-N} = 68.3 °C, T_{N-I} = 113.8 °C) , 3,4,5-trifluoro-4'- (4-propyl- [1,1'-bi (cyclohexan)]-4-yl)-1,1'-biphenyl (3F3) (T_{Cr-N} = 106.3 °C, T_{N-I} = 259.7 °C), 3,4,5-trifluoro-4'- (4-pentyl- [1,1'-bi (cyclohexan)]- 4-yl)-1,1'-biphenyl (5F3) (T_{Cr-N} = 80.1 °C, T_{N-I} = 242.1 °C) and commercial liquid crystal mixture E8 (ordinary refractive index n_o = 1.527, extraordinary refractive index n_e = 1.774, clearing point T_{NI} = 345.2K were supplied by Yan Tai xian hua chemical Technology Co., Ltd. The irgacure 651 was supplied by shanghai Aladdin chemical Technology Co., Ltd. All chemical reagents have not been further purified and the chemical structure is shown in **Figure S**1.
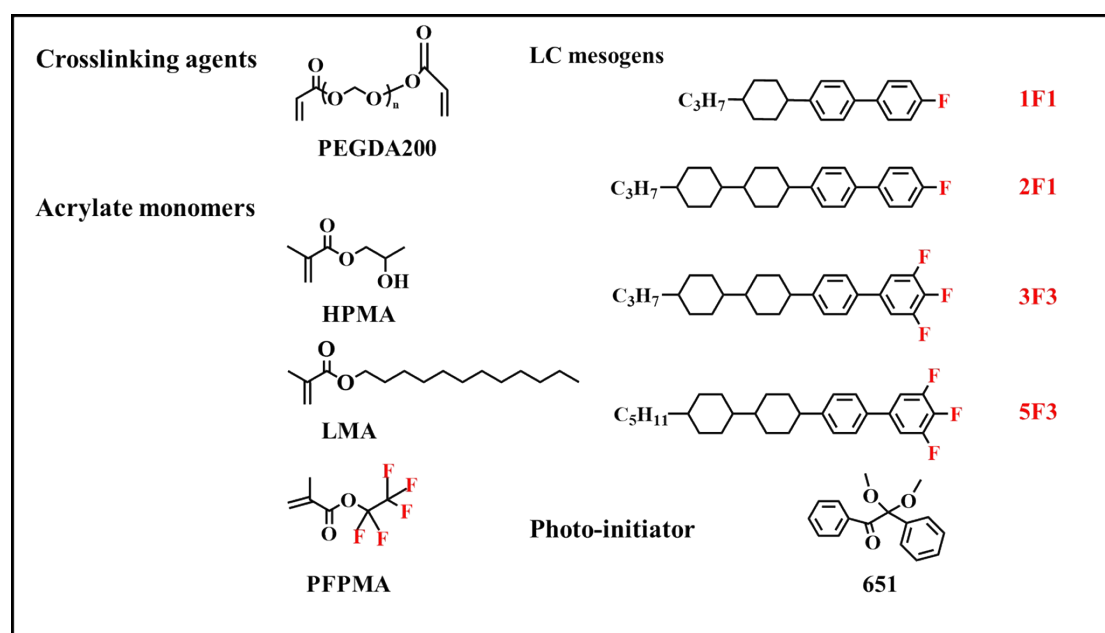

Figure S1. chemical structures of material.

1.2 Measurements

SEM morphology: In order to analyze the structure of the polymer matrix, specimens were fragmented into small segments and immersed in cyclohexane for a duration of 20 days. Given the insolubility of the polymer matrix in the solvent, the liquid crystal (LC) content could be extracted by cyclohexane. Subsequently, the solvent was eliminated by subjecting the samples to heat in an oven at 75 °C for a period of 18 hours. Ultimately, the resultant polymer film was scrutinized through scanning electron microscopy (SEM, JSM-7800F) subsequent to the application of a thin layer of gold onto the surface.

POM: A polarizing optical microscope (POM) manufactured by ZEISS (model: Axio Scope.A1) from Carl Zeiss AG in Oberkochen, Baden Württemberg, Germany, was employed for the examination of the texture of liquid crystal and PDLC films.

DSC: The phase transition temperature of LC mixtures were characterized by a differential scanning calorimeter (Perkin-Elmer DSC 8000) under N_2 atmosphere at a scanning speed of 10.0 °C/min.

Refractive index analysis: The birefringence of the LC mixture ($\Delta n = n_e - n_o$) was investigated by an Abbe refractometer (DR-M2, ATAGO) at 25 °C with sodium light source (589.3nm).

Viscosity analysis: The rotational viscosity (η) of the LC mixture was measured by a digital viscometer (DV-II+ Pro, Brookfield) at 25 °C.

Dielectric constant analysis: The dielectric anisotropy ($\Delta\varepsilon = \varepsilon_{//} - \varepsilon_{\perp}$) of the LC mixture was characterized by a dielectric constant tester (E4980A, Agilent) at 25 °C. where $\varepsilon_{//}$ is the dielectric constant parallel to the long axis of the LC molecules and $\varepsilon_{\perp}$ is the dielectric constant perpendicular to the long axis of the LC molecule.

UV-VIS-NIR spectrum: The UV-VIS-NIR spectrophotometer (PerkinElmer Lambda 950) was used to characterize the transmission spectra of the films. The integral luminous transmittance (Tlum, 380nm-780nm) and solar transmittance (Tsol, 300nm-2500nm) were calculated from the transmittance spectrum of the film according

to the following equations:

$$Tlum = \int \varphi lum(\lambda)T(\lambda)d\lambda / \int \varphi lum(\lambda)d(\lambda) \tag{1}$$

$$Tsol = \int \varphi sol(\lambda)T(\lambda)d\lambda / \int \varphi sol(\lambda)d(\lambda) \tag{2}$$

where $T(\lambda)$ stands for the spectral transmittance, $\varphi lum(\lambda)$ is the standard luminous efficiency function of photopic vision within the wavelength range 380-780 nm. $\varphi sol(\lambda)$ is the solar irradiance spectrum distribution for air mass 1.5 corresponding to the sun standing 37°C above the horizon with 1.5 atm thickness at solar zenith angle of 48.2°. The visible light transmittance variation (ΔT_{lum}) and the solar light modulation ability (ΔT_{sol}) are obtained by the following equations [43-45]:

$$\Delta Tlum = Tlum(on) - Tlum(off) \tag{3}$$

$$\Delta Tsol = Tsol(on) - Tlsol(off) \tag{4}$$

The emissivity spectra within the wavelength range of 2.5 to 14 μm were examined through Fourier transform infrared spectroscopy (FTIR) utilizing the Nicolet iS50 instrument from the United States. As per Kirchhoff's law, it is anticipated that the spectral absorptivity ($\alpha (\lambda)$) and emissivity ($\epsilon (\lambda)$) should be equal for an object in thermal equilibrium. Consequently, the emissivity ($\epsilon (\lambda)$) was calculated as $\epsilon (\lambda) = 1-\rho(\lambda)-\tau(\lambda)$. The values in the long-wave infrared (LWIR) region spanning from 8 to 14 μm were determined using a dual-band emissivity measurement apparatus (IR-2). For each specimen, the LWIR values were measured at six distinct locations, and the mean value was regarded as the ultimate LWIR value. The attenuated total reflection Fourier transform infrared (ATR FTIR) assessments were carried out employing a Nicolet 6700 spectrometer.

The cooling capacity calculations for PRC films are influenced by solar irradiance and atmospheric downward thermal radiation under clear sky conditions. Heat transfer takes place between the PRC films and the surrounding environment, in line with the principle of energy conservation. The net cooling power (P_{net}) can be mathematically represented by the following equation. [38-42].

$$P_{net}(T) = P_{rad}(T) - P_{atm}(T) - P_{sun} - P_{cond + conv} \tag{5}$$

The variable $P_{rad}(T)$ represents the radiation power emitted from the surface of a

radiative cooler in a specific hemisphere, and is determined through a defined mathematical formula:

$$P_{rad}(T) = A \int d\Omega cos\theta \int_{0}^{\infty} d\lambda I_{BB}(T,\lambda)\varepsilon(\lambda,\theta)$$

(6)

Where $\int d = 2\pi \int_{0}^{x} d\theta sin\theta$ represents the angular integral across a hemisphere; The spectral distribution of thermal energy emitted by a blackbody at temperature T is

denoted by $I_{BB}(T,\lambda) = \dfrac{2hc^2}{\lambda^5} \dfrac{1}{e^{hc/(\lambda k_B T)} - 1}$. In this context, h represents Planck's constant, k_B signifies the Boltzmann constant, c denotes the speed of light, and λ stands for the wavelength. The term $\epsilon (\lambda, \theta)$ refers to the spectral and angular emissivity at temperature T. A represents the surface area of the radiative cooler.

$$P_{atm}(T_{amb}) = A \int d\Omega cos\theta \int_{0}^{\infty} d\lambda I_{BB}(T_{amb},\lambda)\varepsilon(\lambda,\theta)\varepsilon_{atm}(\lambda,\theta)$$

(7)

P_{atm} (T_{amb}) represents absorbed power due to incident atmospheric thermal radiation. $\epsilon_{atm}(\lambda,\theta) = 1 - \tau(\lambda)^{1/cos\theta}$, where $\tau(\lambda)$ is the atmospheric transmittance in the zenith direction.

$$P_{solar} = A \int_{0}^{\infty} d\lambda\varepsilon(\lambda,\theta_{solar})I_{AM1.5}(\lambda)$$

(8)

The P_{solar} value signifies the energy absorbed by the film from incoming solar radiation, where $I_{AM1.5}(\lambda)$ represents the standard solar irradiance. The PDLC film, which reflects 90% of solar energy, is anticipated to reduce the daytime cooling capacity by 10% as a result of its solar absorption characteristics.

$$P_{cond+conv}(T,T_{amb}) = Ah_c(T_{amb} - T)$$

(9)

where h_c is combined conduction and convection heating, which is set as 0, 3, 6, 9 and 12 W m^{-2} K^{-1} in this study.

Electro-optical measurement: An LC device parameter tester (LCT-5066C, Chang Chun Liangcheng Instrument Co. Ltd.) was used to examined the electro-optical characteristics at room temperature using 560 nm light. A square-wave modulated

electric field (1000 Hz) was applied. The air transmission is normalized to 100%, whereas the dark transmittance is normalized to 0 %. The distance between the sample and the photodiode is 300 mm. The transmitted light intensity was measured at an angle of around ± 1 degree. The electro-optic performance characteristics of the PDLC film are discussed in depth. The threshold voltage (V_{th}) and saturation voltage (V_{sat}) contribute to 10% and 90% of the maximum transmittance, respectively. The transmittance of the film in the off-state and on-state are denoted by T_{off} and T_{on}, respectively. Contrast Ratio (CR) refers to the ratio of T_{on} to T_{off}. The rise time (T_R) is the time for the transmittance to reach 90% of the on-state transmittance, and the decay time (T_D) is defined as the time for the transmittance to reach 10% of the on-state transmittance, respectively.

Table S1. The compositions of the samples

| Sample | Liquid crystal | | Monomers(wt%) |
	Mixed liquid crystal	Weight ratio(wt%)	
Group A			
A0	E8	70.0	30.0
A1	E8/1F1	50.0/10.0	30.0
A2	E8/2F1	50.0/10.0	30.0
A3	E8/3F3	50.0/10.0	30.0
A4	E8/5F3	50.0/10.0	30.0
Group B			
B0	E8	70.0	30.0
B1	E8/3F3	67.0/3.0	30.0
B2	E8/3F3	64.0/6.0	30.0
B3	E8/3F3	61.0/9.0	30.0

| B4 | E8/3F3 | 58.0/12.0 | 30.0 |
| B5 | E8/3F3 | 55.0/15.0 | 30.0 |

2. Mesh diameter of group A and B

Table S2. Mesh diameter of group A

sample	Mesh diameters distribution (μm)	Average (μm)
A0	0.39-0.66	0.58
A1	0.59-0.78	0.66
A2	1.03-1.64	1.42
A3	0.98-1.77	1.58
A4	1.36-1.97	1.67

Table S3. Mesh diameter of group B

sample	Mesh diameters distribution (μm)	Average (μm)
B0	0.39-0.66	0.58
B1	0.48-1.01	0.62
B2	0.58-1.06	1.80
B3	0.81-1.23	1.01
B4	0.98-1.53	1.21
B5	1.39-2.48	1.78

3. T_{on} and T_{off} of Group A
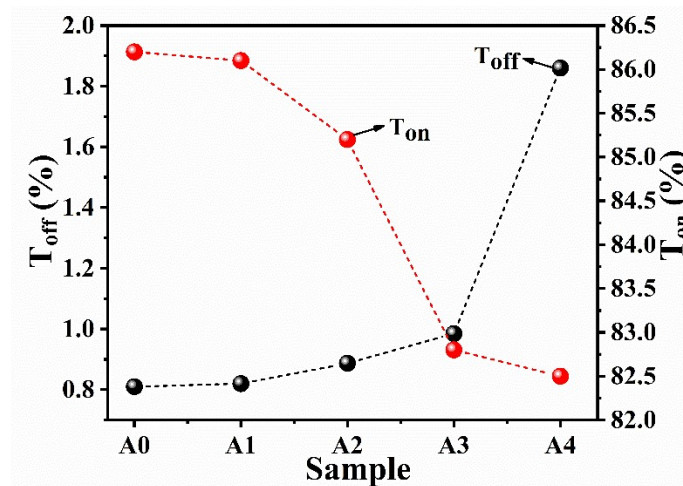
4. Liquid crystal texture and phase transition temperature curve
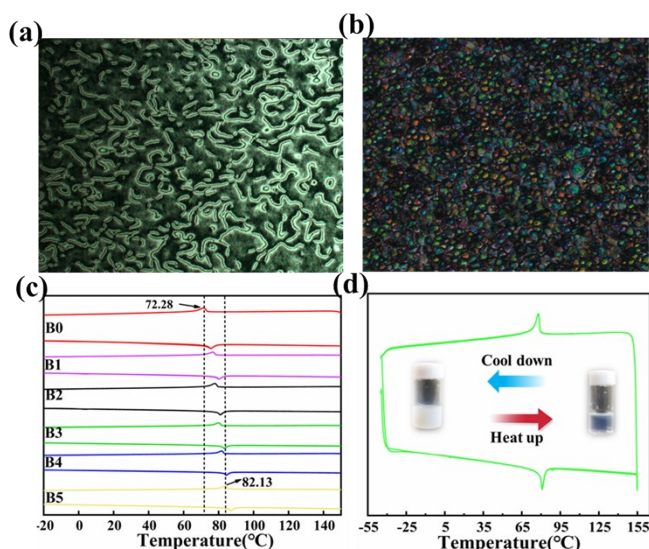

Figure S3. (a-b) Texture of (a) liquid crystal E8/3F3 and (b) PDLC composite film observed by polarized optical microscope under crossed polarizers; (c) DSC curves of LC mixtures B0-B5. (d) DSC curves of LC mixture B3.

5. *Influence of film thickness on the properties of PDLC films.*

Films labeled C0-C2 in thickness of 5μm, 10μm and 20μm, respectively, were prepared to investigate the effect of thickness on the electro-optical properties. The formulations are the same as sample B3 in Table 2. Figure S4(a-c) shows SEM images of films with thicknesses of (a) 5, (b) 10, and (c) 20μm, respectively. It is obvious that the polymer in the 5μm film was relatively sparse, with large polymer mesh. When the film thickness increased from 5μm to 20μm, the polymer exhibited a three-dimensional structure with the densest network configuration. The corresponding cross-sectional images of the samples are shown in Figure S4(d-f). Simultaneously, all samples can achieve the same saturated transmittance level. T_{off} drops with the increase of cell thickness because when the cell thickness is small, the polymer becomes sparse and its

ability to scatter light is reduced in the off state. Consequently, the CR value indicates an ascending trend, as illustrated in Figure S4(h). Moreover, the larger polymer mesh reduced its anchoring force on the LC molecules, thus lowering the driving voltage. The decay time T_D of the samples decreased, while the T_R shows the opposite trend, as shown in Figure S4(i). This is because strong anchoring can facilitate the rapid restoration of the original orientation of liquid crystal molecules (short T_D), but it also results in high resistance to the external electric field (long T_R). **Figure S5** displays the transmittance spectra of the films in different thickness, and the parameters are calculated and listed in Table S4. It can be seen that with the increase of the film thickness, its ability to modulate sunlight decreases slightly.
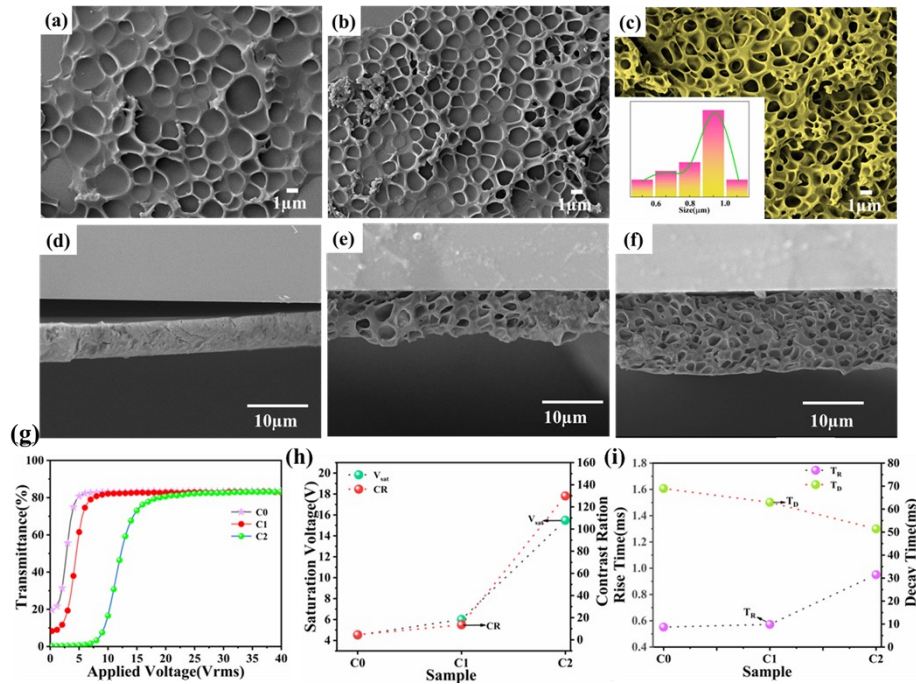

Figure S4. (a-c) longitudinal and (d-f) cross-sectional images of the polymer matrix in PDLC layer of 5μm, 10μm and 20μm; (g) E-O characterization results of sample C0-C2 with different cell thickness; (h) saturation voltage and contrast ration; (i) response time. C0: 5μm, C1:10μm, and C2: 20μm;
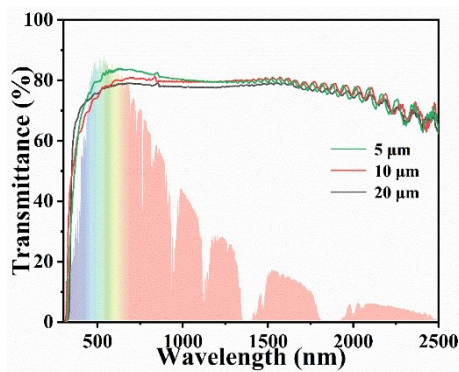
Figure S5. UV-Vis-NIR transmission spectra of films in different thickness;

Table S4. Parameters of PDLC samples in different thickness

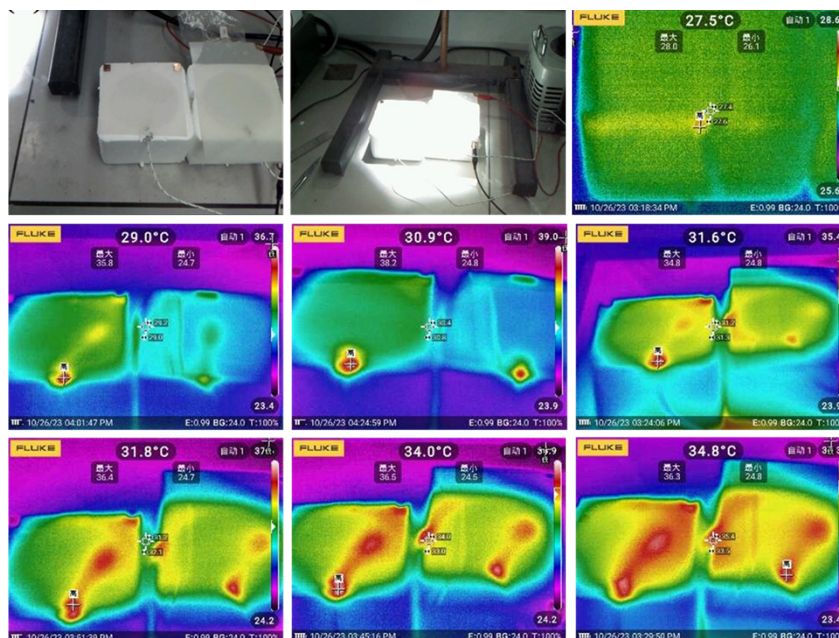| Sample	0V		12V		ΔT_{lum} (%)	ΔT_{sol} (%)
Thickness	T_{lum} (%)	T_{sol} (%)	T_{lum} (%)	T_{sol} (%)		
5μm	1.53	6.03	79.32	73.24	77.79	67.21
10μm	1.46	4.23	77.82	71.24	76.36	67.01
20μm	1.29	3.28	76.42	69.69	75.13	66.41

6. Xenon lamp simulated irradiation test

Figure S6. Irradiation simulation test and infrared thermal images